JOURNAL OF GEOPHYSICAL RESEARCH, VOL. 112, A06237, doi:10.1029/2006JA012030, 2007

Plasmaspheric drainage plume observed by the Polar satellite in the prenoon sector and the IMAGE satellite during the magnetic storm of 11 April 2001

K.-H. Kim,[1] J. Goldstein,[2] and D. Berube[3]

Received 20 August 2006; revised 25 February 2007; accepted 6 March 2007; published 21 June 2007.

[1] During the early main phase of a geomagnetic storm on 11 April 2001, the Polar satellite was inside the magnetosphere in the prenoon sector (~1000–1100 magnetic local times) and experienced a magnetopause crossing at $L \approx 6$ because of the high solar wind dynamic pressure and strong southward interplanetary magnetic field (IMF). Just before the magnetopause crossing, Polar observed cold, dense plasma. That is, the cold, dense plasma was immediately adjacent to the compressed magnetopause. Using simultaneous observations by the IMAGE extreme ultraviolet (EUV) imager, we confirm that the cold, dense plasma observed by Polar is a plasmaspheric drainage plume extending outward from the plasmasphere to the magnetopause during the interval of high geomagnetic activity and strong southward IMF. We compare plasmaspheric mass densities determined from ground magnetometer data at $L = 2.3$ and 2.9 for a magnetically quiet time interval to mass densities determined during the magnetic storm time interval. We find no significant differences in the mass density between both intervals. These observations suggest that the sunward-convecting plasmaspheric plasma observed at Polar is due to erosion of the outer layers of the plasmasphere beyond $L = 2.9$.

Citation: Kim, K.-H., J. Goldstein, and D. Berube (2007), Plasmaspheric drainage plume observed by the Polar satellite in the prenoon sector and the IMAGE satellite during the magnetic storm of 11 April 2001, *J. Geophys. Res.*, *112*, A06237, doi:10.1029/2006JA012030.

1. Introduction

[2] The plasmasphere is a region of dense (~10^2–10^4 cm^{-3}), cold (~1 eV) plasma surrounding the Earth in the innermost part of the magnetosphere. This region typically extends out to several Earth radii from the ionosphere along the magnetic equator. The plasmasphere is bounded by a sharp density gradient region, called the plasmapause, where the density can drop by 1–2 orders of magnitude over a region of less than 0.5 L. A variety of ground-based and space-based studies have contributed to our understanding of the global picture of the plasmasphere and its dynamics [see *Lemaire and Gringauz*, 1998].

[3] Since the plasmapause is formed by the influences of both the solar-wind-driven convection electric field and the electric field associated with the Earth's rotation, the size and shape of the plasmasphere depend considerably on the level of magnetospheric activity and the interplanetary magnetic field (IMF) conditions. Previous studies reported that the radial location of the plasmapause varies inversely with the level of geomagnetic activity [e.g., *Carpenter*, 1967; *Chappell et al.*, 1970]. Under quiet conditions, the plasmasphere extends beyond geosynchronous orbit [e.g., *Moldwin et al.*, 1994; *Spasojević et al.*, 2003]. During times of high geomagnetic activity, the outer part of the plasmasphere experiences erosion and the plasmapause moves earthward, as far inward as $L < 3$ [e.g., *Carpenter and Anderson*, 1992; *Moldwin et al.*, 2002].

[4] Recently, new observations of the plasmasphere have been made by the Extreme Ultraviolet (EUV) imager [*Sandel et al.*, 2000] on board the IMAGE satellite [*Burch*, 2000]. The IMAGE/EUV data provide global images of the plasmasphere and show many cases of plasmaspheric erosions during southward IMF intervals. The dynamic behavior of the plasmapause during these erosion events follows a consistent and repeatable pattern; the nightside plasmapause moves sunward/earthward and the dayside plasmapause moves sunward forming a sunward extending plume from the main plasmasphere into the outer magnetosphere [e.g., *Spasojević et al.*, 2003; *Goldstein et al.*, 2004b, 2005; *Goldstein and Sandel*, 2005].

[5] The average plasmaspheric distribution at geosynchronous orbit peaks near 1800 local time (LT) because of the plasmaspheric duskside bulge [e.g., *Carpenter et al.*, 1993]. The bulge plasma moves to earlier local times (i.e., toward noon) with increasing geomagnetic activity [*Higel and Wu*, 1984; *Moldwin et al.*, 1994]. The evolution of the plasmaspheric bulge location in local time with changing

[1] Korea Astronomy and Space Science Institute, Daejeon, Korea.
[2] Space Science and Engineering Division, Southwest Research Institute, San Antonio, Texas, USA.
[3] Department of Earth and Space Sciences, University of California, Los Angeles, California, USA.

0148-0227/07/2006JA012030$09.00

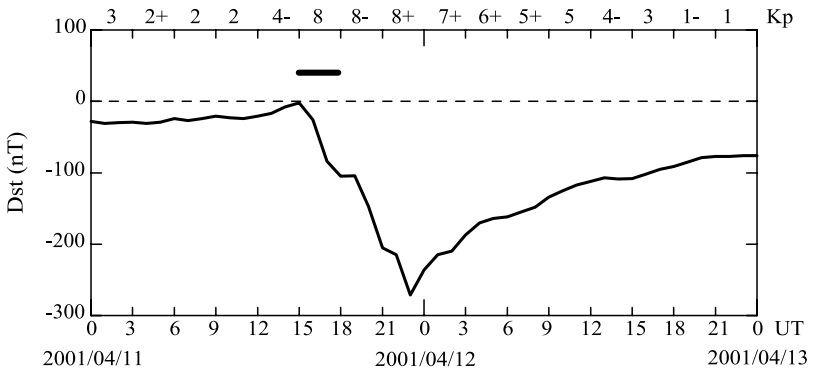

Figure 1. *Dst* index during 11–12 April 2001. The horizontal bar indicates the interval of 1500–1800 UT on 11 April 2001 when the Polar satellite experienced different plasma regimes (i.e., outer magnetosphere, plasmasphere, and magnetosheath).

geomagnetic activity can be expected from theoretical models [e.g., *Grebowsky*, 1970]. However, duskside plasmaspheric structures are more complicated than what the models expect [*Carpenter et al.*, 1993].

[6] Plasmaspheric material on high-latitude open field lines has been reported by *Su et al.* [2001]. The authors suggest that draining plasmaspheric plasma can be expected on reconnected field lines when the convection electric field suddenly increases and that the plasmaspheric material can be transported on high-latitude reconnected field lines. These thermal ion events have been observed in the dayside outer magnetosphere beyond geosynchronous orbit, occurring more frequently at the duskside than at the dawnside [*Chen and Moore*, 2006]. The events were interpreted as the result of plasmaspheric drainage plumes extending from the dusk region near geosynchronous orbit toward the magnetopause. Plasmaspheric plasma is often observed following crossings of the compressed magnetopause at geosynchronous orbit during and/or after geomagnetic disturbances, and its local-time-occurrence distribution is skewed sunward (peaking near 1400 LT with a local time range from 1000 to 1800 LT) [*Elphic et al.*, 1996]. Such geosynchronous observations of plasmaspheric plasma adjacent to the compressed magnetopause on the dayside are considered to be signatures of plasmaspheric plumes extending sunward from the main plasmasphere during intervals of enhanced magnetospheric convection.

[7] Observations of plasmaspheric plasma adjacent to the compressed dayside magnetopause have mainly been reported using geosynchronous orbit data [e.g., *Elphic et al.*, 1996]. Simultaneous IMAGE/EUV and in situ observations of drainage plumes at geosynchronous orbit have already been reported [e.g., *Goldstein et al.*, 2004b]. However, there are no simultaneous remote sensing and in situ observations of plasmaspheric drainage plumes attached to the compressed magnetopause inside geosynchronous orbit in the prenoon sector. In this paper, we show the cold, dense plasma observed by the Polar satellite in the prenoon sector (~1000–1100 magnetic local times) and at $L \approx 6$ just before the magnetopause crossing during the early main phase of the geomagnetic storm on 11 April 2001. Using simultaneous observations by IMAGE/EUV, we show that the cold, dense plasma adjacent to the compressed magnetopause is a plasmaspheric drainage plume extending outward from the plasmasphere to the magnetopause.

2. Observations

2.1. Overview of the Selected Interval

[8] Figure 1 shows hourly averages of the *Dst* index throughout the time interval from 11 April to 12 April 2001. From the *Dst* index we see that the magnetic storm started at 1500 UT on 11 April, and during the main phase of the storm, *Dst* monotonically decreased to −270 nT and then gradually began to recover. On the top of Figure 1, the 3-hour values of the *Kp* index are displayed. The main phase of the storm was characterized by extremely disturbed geomagnetic activity with *Kp* values of 8− to 8+. In this paper, we focus on the time interval from 1500 to 1800 UT (marked by the horizontal bar in Figure 1) when Polar observed cold, dense plasma just inside a highly compressed magnetopause.

[9] Figures 2a–2c show the solar wind dynamic pressure, the IMF B_z in GSM (geocentric solar magnetospheric) coordinates observed by the ACE spacecraft, and the GOES 8 B_H component (northward), antiparallel to the magnetic dipole axis in VDH coordinates, for the interval from 1430 to 1800 UT on 11 April 2001. At geosynchronous orbit, on the dayside, B_H is nearly equal to the total magnetic field magnitude (i.e., $B_H \approx |B|$). Thus, the magnetospheric response (compression or expansion) to solar wind dynamic pressure variations can be examined by looking at B_H. During this interval, ACE was located near GSE $(x, y, z) \sim (221.3, -8.9, -19.5)$ R_E, and GOES 8 moved through its geosynchronous orbit from 0930 to 1300 hours magnetic local time (MLT). ACE detected the passage of an interplanetary shock at 1528 UT. At the time of the shock passage, the dynamic pressure exhibited a step-like transition from ~10 to ~20 nPa. Following the arrival of the shock, IMF B_z became more strongly negative (−30 nT) than before 1528 UT. Note that the southward turning of IMF occurred at ~1445 UT and a stronger southward enhancement was observed at ~1451 UT. Although there were several intervals of northward IMF, ACE mainly observed strong southward IMF during the 1430–1800 UT interval. These solar wind conditions

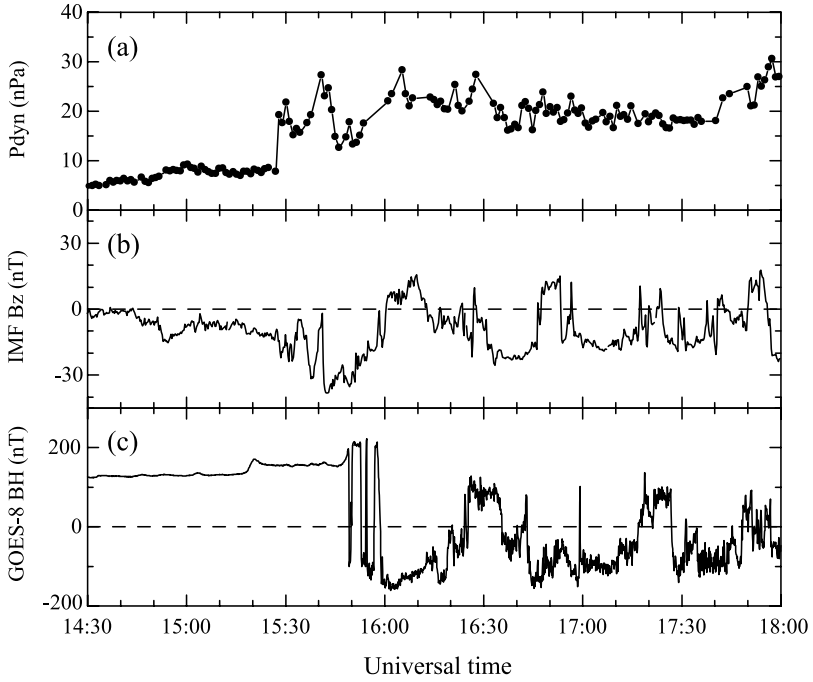

Figure 2. (a) Solar wind dynamic pressure and (b) interplanetary magnetic field B_z component measured by the ACE satellite. (c) GOES 8 magnetic field data in the BH component, which is antiparallel to the Earth's dipole axis, in VDH coordinates.

enhanced magnetospheric convection and caused the major geomagnetic storm on 11 April 2001.

[10] About 20 min after the time of the step-like pressure increase at ACE, GOES 8, near the subsolar region, observed a sudden increase in the magnitude of B_H and experienced several magnetopause crossings. From this 20-min time lag, we expect that the sudden increase in B_H at ~1518 UT is due to the solar wind dynamic pressure increase at ~1459 UT [*Taguchi et al.*, 2004]. After 1600 UT, GOES 8 entered the magnetosheath and observed turbulent magnetosheath magnetic field variations. These magnetospheric responses at geosynchronous orbit are due to the inward motion of the magnetopause as a result of strongly enhanced solar wind dynamic pressure variations which began at 1528 UT. That is, the interplanetary shock resulted in a rapid compression of the magnetosphere to within geosynchronous orbit. We note that the 20-min time delay between ACE and GOES 8 is shorter than the estimated time lag, ~35 min, using the observed solar wind speed of ~650 km/s (data not shown here). The shorter lag may be due to the discontinuity front, which is tilted from the Sun-Earth axis [*Taguchi et al.*, 2004].

2.2. Plasmaspheric Plasma Observed by Polar

[11] Figure 3 illustrates the Polar orbit for the interval of 1500–1800 UT in solar magnetic (SM) coordinates. The spacecraft positions are plotted onto the SM *x*-*z* and *x*-*y* planes, with solid lines marked every hour by open circles. During this interval, Polar was located near the prenoon sector from 1000 to 1100 MLT and below the magnetic equator. The heavy portion of the orbit trace indicates the intervals when the spacecraft measured cold, dense (electron density >100 cm^{-3}) plasmaspheric plasma. Polar exited the dense plasma at $L \approx 6$ as it crossed the magnetopause and experienced different plasma regimes because of solar wind dynamic pressure variations and strong southward IMF B_z during the main phase of the magnetic storm, as we will show below.

[12] Figure 4a shows the magnetic field data observed by Polar for the 3-hour interval, 1500–1800 UT. The magnetic field data are presented in the B_H component in VDH coordinates. The dashed curve in Figure 4a represents the model B_H determined by the IGRF2000 magnetic field model, provided at http://www-spof.gsfc.nasa.gov/Modeling/geopack.html. The difference between the observed B_H and model B_H field intensities from ~1547 to ~1657 UT, marked by the vertical dashed lines labeled "1" and "3", indicates that the magnetosphere was compressed, as expected from the passage of the interplanetary shock. We note that the magnetic compression at ~1547 UT occurred nearly simultaneously at GOES 8 and Polar. B_H rotated from northward to southward at ~1657 UT, marked by the vertical dashed line labeled "3", indicating that Polar crossed the magnetopause. Just after the magnetopause crossing at ~1657 UT, Polar observed transient magnetopause crossings because of radial magnetopause motions and then entered the magnetosheath. The magnetic field strength remained enhanced until the satellite crossed the magnetopause, indicating that Polar was inside the compressed magnetosphere. During the interval of ~1657–1800 UT, Polar was in the magnetosheath and observed turbulent magnetosheath magnetic field variations.

[13] Figure 4b shows the electron density (N_{sp}) inferred from the spacecraft potential [*Scudder et al.*, 2000] and the Hydra particle detector [*Scudder et al.*, 1995]. Since the

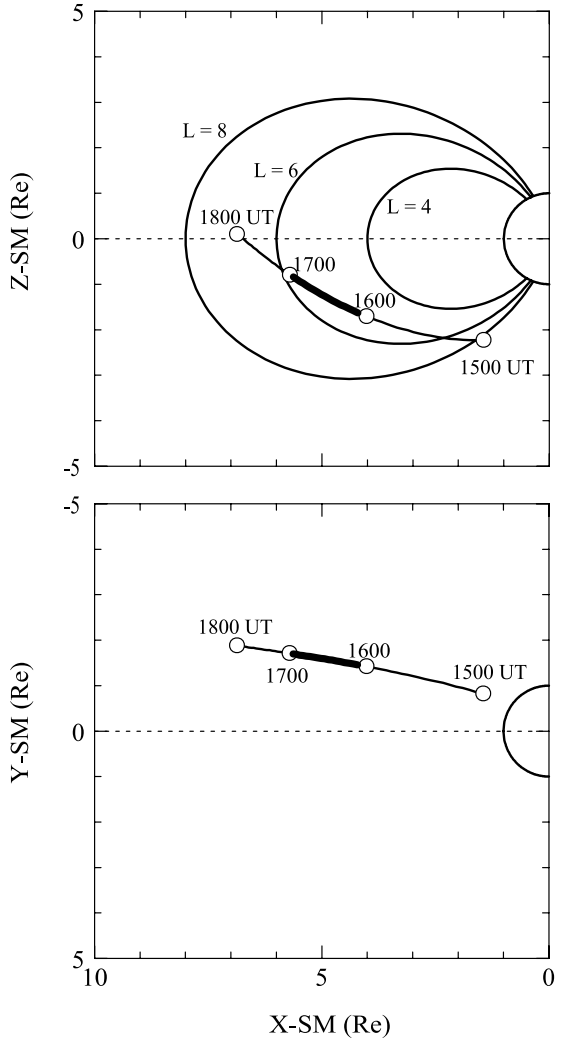

Figure 3. Orbit of the Polar satellite for the interval of 1500–1800 UT on 11 April 2001. The orbit is projected onto the solar magnetic (upper panel) *x-z* plane and (lower panel) *x-y* plane. The open circles indicate the hourly position of the satellite. Region of high-density plasma (i.e., the plasmasphere) is indicated by thick line segments.

result of *Scudder et al.* [2000] was obtained using the data of ~10 months during solar minimum (April 1996 to March 1997), one might question whether the result can be applied for our event on 11 April 2001 during solar maximum. It is noteworthy that the density calculation from the measured spacecraft potential is only accurate to about a factor of 2 [*Pedersen*, 1995]. Therefore our N_{sp} is at best an order of magnitude estimate of electron density. Polar observed low-density plasma ($N_{sp} < \sim 10$ cm^{-3}) until 1609 UT and then dense plasma ($N_{sp} > 100$ cm^{-3}) from 1611 UT, marked by the vertical dashed line labeled "2", until just before the magnetopause crossing at 1657 UT. Since the spacecraft potential is also affected by particle flux, the dense plasma encountered by Polar before the magnetopause crossing could be due to an increase in particle energy flux [e.g., *Keiling et al.*, 2001]. In Figure 4c, however, the Hydra particle instrument detected a sharp flux decrease from 1611 to 1657 UT. Thus the N_{sp} increase is not due to the increase of the energetic particle flux but the increase of the low-energy particles below the energy cutoff (12 eV) of Hydra (i.e., cold plasmaspheric plasma). The significant difference between N_{sp} and Hydra electron density for the interval 1611–1657 UT indicates that Polar encountered plasmaspheric plasma.

[14] A sharp flux increase of electrons between a few tens of electron volts and ~100 eV beginning at ~1520 UT in Figure 4c is due to magnetospheric compression (see also Figure 2), and the stronger compression at ~1547 caused a flux increase over the whole energy range. These flux increases are explained as an adiabatic response of electrons. The magnetosheath plasma distribution is readily identified between 1657 and 1800 UT. This interval is characterized by very intense electron fluxes from several tens of electron volts to several hundred electron volts. During the interval 1611–1657 UT, Polar transiently observed magnetosheath plasma. There were no significant magnetic field variations during these transient events, except for the event at ~1627 UT. This indicates that Polar briefly entered the boundary layer region at ~1630, ~1635, and ~1643 UT and the magnetosheath at ~1627 UT from the plasmaspheric plasma region. We cannot identify bursty events of the plasmaspheric plasma in the magnetosheath region. Therefore one may argue that the plasmaspheric material appears to remain within the magnetosphere rather than streaming into the solar wind. However, we do not exclude the possibility that the plasmaspheric material becomes accelerated by reconnection and mixed with solar wind plasma at the magnetopause [*Elphic et al.*, 1997; *Su et al.*, 2000].

2.3. Plasmaspheric Drainage Plume Observed by IMAGE/EUV

[15] On the basis of theoretical studies [e.g., *Grebowsky*, 1970] and previous observational works [e.g., *Elphic et al.*, 1996], it might be expected that the cold, dense plasma observed by Polar just inside the magnetopause is sunward-convecting plasmaspheric plasma associated with high geomagnetic activity and an increase in the magnitude of southward IMF. Such sunward motion can be inferred from global plasmaspheric images captured by the IMAGE/EUV instrument [e.g., *Goldstein and Sandel*, 2005; *Goldstein et al.*, 2004a; 2004b]. IMAGE/EUV maps the distribution of He^+ in the plasmasphere by imaging 30.4-nm sunlight resonantly scattered by plasmaspheric He^+ ions [*Sandel et al.*, 2000, 2001]. The He^+ portion corresponds to total number densities above about 40 cm^{-3} [*Goldstein et al.*, 2003b].

[16] Figure 5 shows the locations of the plasmapause (dotted circles) extracted from the IMAGE/EUV images [*Goldstein et al.*, 2003b] in the *L*-MLT plane at three different times on 11 April 2001. There are gaps in the extracted plasmapause locations where no plasmapause was identifiable, owing to noise or sunlight contamination. Some details of instrument artifacts are described by *Goldstein et al.* [2004a]. From a series of plasmapause shapes in Figure 5 we can see that a plasmaspheric erosion is underway. The plasmapause at 1512 UT had a smooth nightside shape with midnight plasmapause location at $L = 4$ and an irregularly shaped dayside structure with noon-sector plasmapause at $L = 3–4$. At 1512 UT, Polar

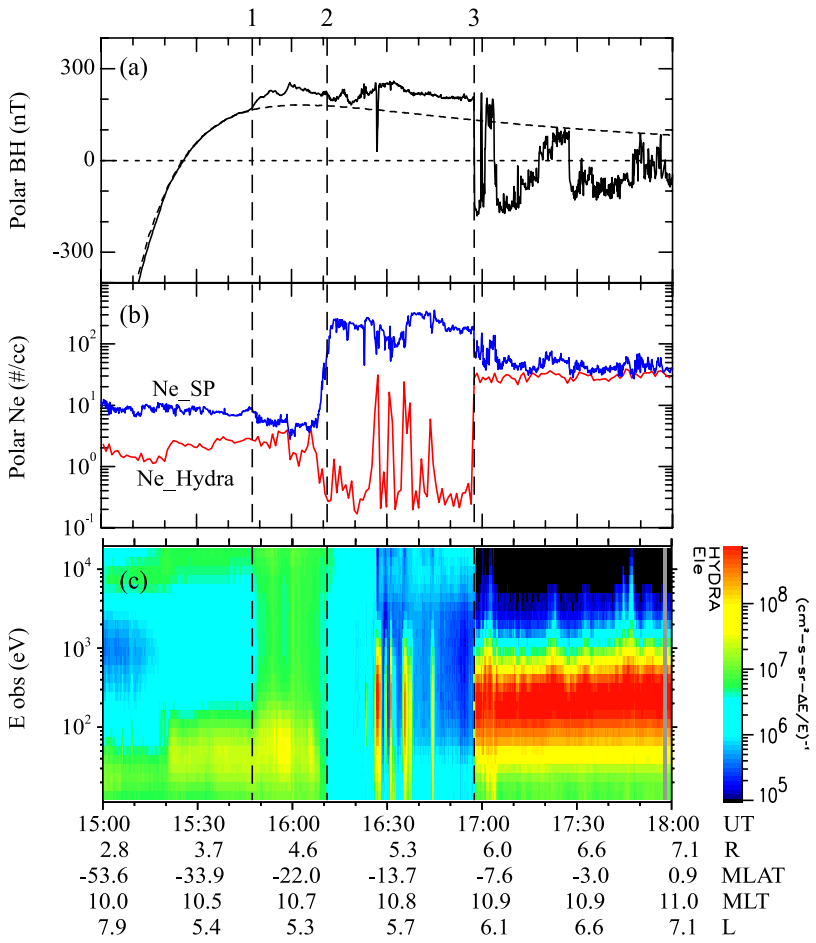

Figure 4. (a) Polar magnetic field data (solid line) and model magnetic field (dashed curve line) in the B_H component, which is antiparallel to the Earth's dipole axis, in VDH coordinates. (b) Electron density (blue) determined from the spacecraft potential and electron density (red) determined from the Hydra particle data. (c) Energy-time spectrogram of electrons.

(open circle) was located at a radial distance of 3.2 R_E, a magnetic latitude of −44.2, and L = 6.2. Polar was outside the plasmasphere and observed plasma density of about 10 cm^{-3}. In Figure 5b, the midnight-sector plasmapause moved inward to L = 3 and the noon-sector plasmapause expanded outward, that is, the dayside plasmaspheric plasma surged sunward, forming a broad dayside plume [*Spasojević et al.*, 2003; *Goldstein et al.*, 2004b; *Goldstein and Sandel*, 2005]. Because the sunward plasmapause (boundary) motion (on both dayside and nightside) agrees with predictions of theoretical models [e.g., *Grebowsky*, 1970] in which this boundary motion results from sunward

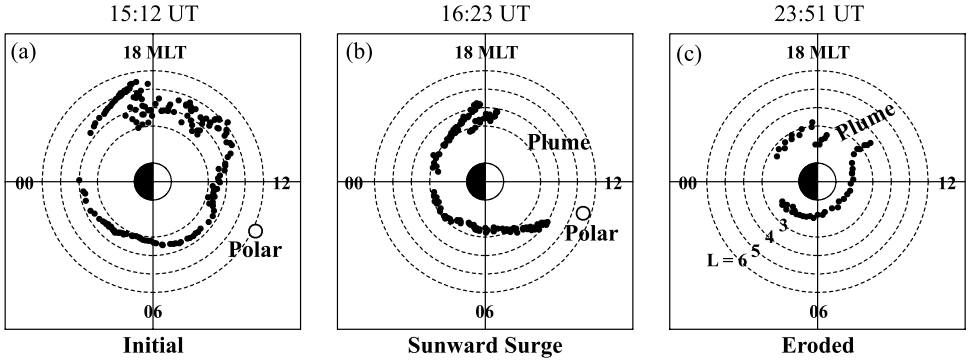

Figure 5. The dotted circles are the locations of the plasmapause extracted from the IMAGE/EUV images. The open circle in left and middle panels indicates the Polar's location at 1512 and 1623 UT, respectively.

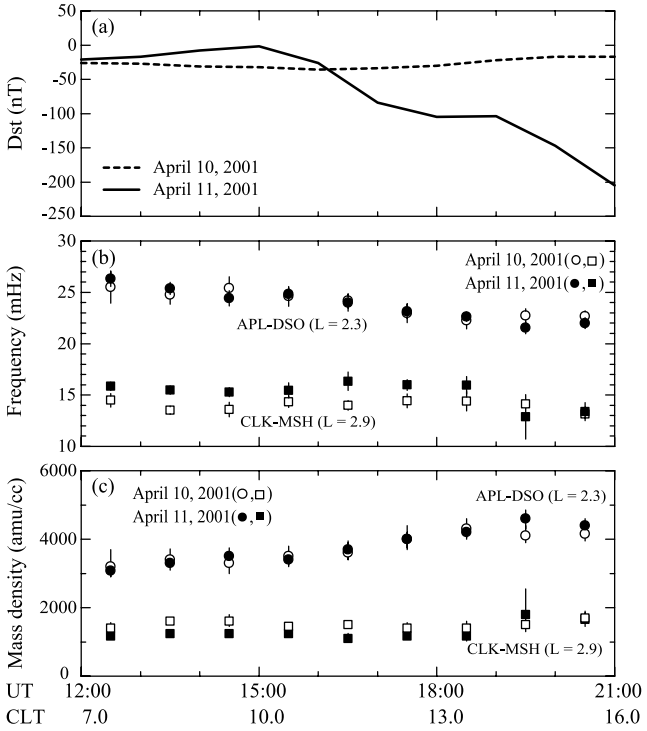

Figure 6. (a) *Dst* index during 1200–2100 UT on 10 April 2001(dashed line) and on 11 April 2001 (solid line). (b) Fundamental mode frequencies of field line resonances (FLR) at $L = 2.3$ and $L = 2.9$ from ground observations. (c) Equatorial plasma mass densities estimated from the observed FLR frequencies in the middle panel. The local time of Clarkson (CLT) is shown at the bottom.

plasma convection, it is likely that the IMAGE-observed plasmapause motion is the result of such sunward convection. Furthermore, because Polar had (at 1623 UT) just crossed the western edge of the IMAGE-observed plume, it follows that the cold plasma seen by Polar was convecting sunward. Thus, we conclude that the cold, dense plasma observed by Polar is sunward moving and part of the global plume structure. At 2351 UT, after several hours of erosion, the plasmasphere was extremely eroded with nightside plasmapause at $L = 2.5$, and the broad dayside plume was narrowed to a width of just a few hours in local time in the predusk sector. This configuration is typical of late-stage plasmaspheric erosion [*Goldstein and Sandel*, 2005]. At this time, Polar was at $L = 10.6$, and thus the location of Polar is not plotted in Figure 5c.

2.4. Mass Density Based on Field Line Resonance Frequency

[17] In order to examine the plasma density variations inside the plasmapause determined by IMAGE/EUV, we compare the plasma mass densities at $L = 2.3$ and 2.9 during the storm time interval and a geomagnetically quiet time interval, respectively. Figure 6a shows the *Dst* index during the interval from 1200 to 2100 UT on 10 and 11 April 2001. The *Dst* change on 11 April 2001 indicates that the magnetic storm started at 1500 UT and the main phase continued until 2100 UT, while on 10 April 2001, the *Dst* index was relatively constant with a variation between −17 and −40 nT, and the *Kp* index was 2–3 for the 9-hour interval, indicating that the interval was not associated with an unusual geomagnetic activity.

[18] The plasmaspheric plasma mass density in the vicinity of the magnetic equator can be determined from field line resonance frequencies measured by magnetometers on the Earth's surface. The ground-based data used in this paper are from four stations (two pairs) in the MEASURE (Magnetometers Along the Eastern Seaboard for Undergraduate Research, http://measure.igpp. ucla.edu/getdata.php) ground magnetometer array. The stations are listed in Table 1. The time interval between 1200 and 2100 UT corresponds to the 0700–1600 local time interval in the MEASURE array.

[19] The fundamental field line resonance (FLR) frequencies of the magnetic field line at $L = 2.3$ for Applied Physics Lab. (APL)-Darksky Observatory (DSO) pair and $L = 2.9$ for Clarkson (CLK)-Millstone Hill (MSH) pair, determined using the automated cross-phase technique [*Berube et al.*, 2003, and references therein], are plotted in Figure 6b. We note that the FLR frequencies were observed during the interval from 1200 to 2100 UT when the ground stations were on the dayside. The FLR frequencies at $L = 2.3$ for 11 April are similar to those for 10 April. There is a tendency

Table 1. List of MEASURE Stations Used in This Study

Station	Code	Geographic Latitude	Geographic Longitude	*L*	LT
Clarkson	CLK	44.7°	285.0°	3.1	UT-5.0
Millstone Hill	MSH	42.6°	288.5°	2.8	UT-4.8
Applied Physics Lab.	APL	39.2°	283.1°	2.4	UT-5.1
Darksky Observatory	DSO	36.3°	278.6°	2.2	UT-5.4

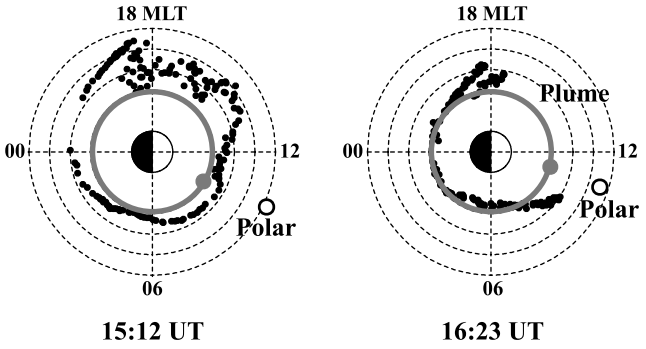

Figure 7. The format is the same as Figure 5, but the locations of the CLK-MSH pair at 1512 UT and 1623 UT are plotted with gray dots. The gray circle line is drawn at $L = 2.9$, which is the magnetic shell parameter of the CLK-MSH pair.

for the FLR frequencies at $L = 2.3$ to decrease monotonically throughout the day, i.e., slightly higher in the morning than in the afternoon. This morning/afternoon asymmetry has been reported in previous studies [e.g., *Waters et al.*, 1994; *Chi et al.*, 2000; *Berube et al.*, 2003] and interpreted as ion outflow from the ionosphere into the equatorial plasmasphere on the dayside. Unlike the FLR signature at $L = 2.3$, on 11 April the FLR frequencies at $L = 2.9$ increase slightly for several hours from 1600 to 1900 UT before decreasing again later in the afternoon. The 1600–1900 UT interval covers the plasmaspheric drainage observed at Polar and is during the main phase of the magnetic storm. Since Polar and the ground stations were in the prenoon sector (near 11-hour local time) with a small local time separation (within 1 hour) for the 1600–1700 UT interval as shown in Figure 7, the increase of the FLR frequency would indicate a decrease in plasma mass density at $L = 2.9$ because of the sunward-convecting plasmaspheric plasma. However, the trend of FLR variations at $L = 2.9$ during the main phase of the magnetic storm was similar to that during quiet time (10 April). Therefore we suggest that the increase in the FLR frequencies for the 1600–1900 UT interval at $L = 2.9$ on 11 April is not a storm-related phenomena. It is not clear what causes different diurnal variations of the FLR frequency at $L = 2.3$ and 2.9, and more studies are needed to understand the cause of their difference.

[20] The plasma mass densities corresponding to the FLR frequencies are calculated using the toroidal mode equation of *Cummings et al.* [1969]. The results are shown in Figure 6c for $L = 2.3$ and $L = 2.9$. The inferred mass density was between ~3000 and ~4000 amu/cm^3 for $L = 2.3$ and between ~1000 and ~2000 amu/cm^3 for $L = 2.9$. These values are comparable to those in recent studies [*Berube et al.*, 2003, 2005]. As expected from the FLR frequencies, the inferred densities on quiet day (10 April) are similar to those during the main phase of the magnetic storm on 11 April. These observations suggest that there is no significant plasmaspheric erosion at $L < 2.9$ during the main phase of the geomagnetic storm from 1500 to 2100 UT on April 11. This indicates that the plasmaspheric plume observed by IMAGE/EUV at 1623 UT (see Figures 5 and 7) and the cold, dense plasma observed at Polar (see Figure 4) during 1611–1657 UT should be the plasmaspheric plasma stripped away from outer layers ($L > 2.9$) of the plasmasphere.

3. Discussion and Summary

[21] A previous study by *Elphic et al.* [1996] reported that plasmaspheric plasma is occasionally observed on the dayside just before geosynchronous magnetopause crossings during geomagnetic storms. The authors suggested two ways to explain the appearance of plasmaspheric plasma at geosynchronous orbit; one is the inward motion of the plasmaspheric plasma, which is already in the outer magnetosphere, because of magnetospheric compression, and the other is the sunward convection of the dayside plasmaspheric plasma because of an enhanced convection electric field. Although *Elphic et al.* [1996] identified the plasmaspheric plasma with multipoint measurements at geosynchronous orbit, it was not easy to identify how and where the plasmaspheric plasma establishes in the outer magnetosphere.

[22] We have shown the cold, dense plasmaspheric plasma observed by Polar in the prenoon sector (~1000–1100 MLT) of the outer magnetosphere just before a magnetopause crossing at $L \approx 6$ during the early main phase of the geomagnetic storm on 11 April 2001. The plasmaspheric plasma was immediately adjacent to the strongly compressed magnetopause. Thus, our event is similar to the events discussed in the work of *Elphic et al.* [1996]. Using the simultaneous global plasmaspheric images of IMAGE/EUV, we confirmed that the cold, dense plasma observed by Polar is the plasmaspheric drainage plume associated with plasmaspheric erosion. Although many observations of plasmaspheric plumes have been reported using global plasmaspheric images [e.g., *Sandel et al.*, 2001; *Goldstein et al.*, 2003a, 2003b; *Spasojević et al.*, 2003; *Goldstein et al.*, 2004b; *Goldstein and Sandel*, 2005], there are no simultaneous remote sensing and in situ observations of plasmaspheric drainage plume attached at the compressed magnetopause in the prenoon sector to the authors' knowledge. Since plasmaspheric erosion is strongly correlated with the solar wind and IMF conditions [e.g., *Carpenter et al.*, 1993; *Carpenter and Lemaire*, 1997; *Goldstein et al.*, 2003b; *Spasojević et al.*, 2003], our observations may be due to strong southward IMF with maximum deflections to −30 nT and strong magnetospheric compression which caused the dayside magnetopause to move inward by ~6 R_E.

[23] In order to examine the relationship between the solar wind/IMF conditions and dynamic behavior of the plasmasphere, we plot the solar wind speed (V_{SW}) and IMF B_z from ACE time shifted by 20 min, the average plasmapause locations in the local time sectors $3 < MLT < 4$ and $9 < MLT < 10$ from all available EUV images from 1430 to 1645 UT and the plasmaspheric plasma attached to the magnetopause observed by Polar in Figure 8. A southward IMF turning reached the magnetopause at ~1504 UT and lasted about 80 min with transient northward turnings at ~1554 UT and ~1601 UT. According to recent studies [*Goldstein and Sandel*, 2005, and references therein], inward motion of the nightside plasmapause occurs ~20–30 min after the arrival of southward IMF at the dayside magnetopause. Therefore we expect that plasmaspheric erosion begins at ~1530 UT.

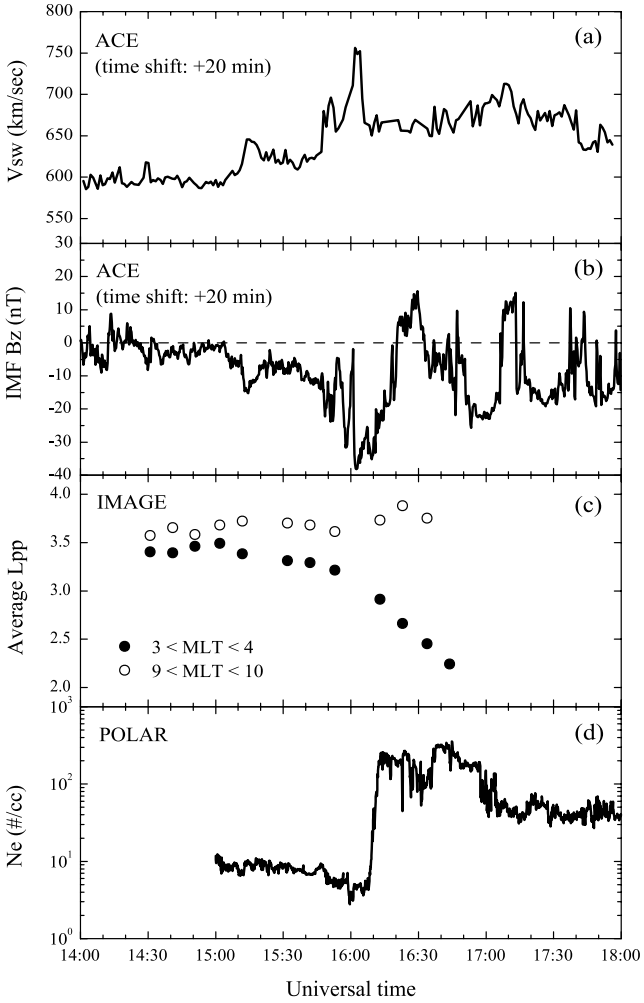

Figure 8. (a) Solar wind speed and (b) interplanetary magnetic field B_z component from the ACE satellite time shifted by 20 min. (c) The average plasmapause locations in L (L_{pp})between 3 and 4 MLT (solid circles) and between 9 and 10 MLT (open circles) from the IMAGE/EUV images. (d) Electron density determined from the spacecraft potential of the Polar satellite.

[24] An interesting feature is that the average erosion rate of the nightside plasmapause (3 < MLT < 4) significantly increased after dramatic increase in the magnitude of southward IMF and V_{SW} at ~1550 UT. The average erosion rate from ~1550 to ~1650 UT was 1.14 L per hour, which is much larger than during a weak geomagnetic disturbance interval reported by *Spasojević et al.* [2003]. Such a sudden increased erosion rate may be due to a combination of a strong southward IMF and an increase in the magnitude of the solar wind speed [*Goldstein et al.*, 2003a]. The rate of erosion is related to the strength of magnetospheric convection, which is proportional to a duskward solar wind electric field, $E_{SW} = V_{SW}B_{z,IMF}$. Of particular interest in Figure 8 is the fact that the average plasmapause location in the morning (9 < MLT < 10) sector increased at ~1610 UT when the cold, dense plasma was observed by Polar in the outer magnetosphere. This outward motion of the morning-side plasmapause may be interpreted as sunward surge of the plasmaspheric plasma creating a broad drainage plume on the dayside. Our observations suggest that the density enhancement seen by Polar is not a static structure. That is, Polar did not pass through a stationary plume; rather a sunward surge, forming a broad plasmaspheric drainage plume, overtook Polar's location in the prenoon sector.

[25] During geomagnetic storms, plasmaspheric plasma density decreases because of an erosion of the plasmasphere by enhanced convection. Recently, plasmaspheric depletions at $L < 3$ during the recovery phase of geomagnetic storms have been reported by *Chi et al.* [2000] and *Reinisch et al.* [2004]. During the main phase of the large magnetic storms on 29–31 October 2003, *Chi et al.* [2005] observed strongly enhanced equatorial mass densities inferred from FLR frequency at $L = 2.5$ and 3. The authors suggested that the density enhancement is due to the penetration of the enhanced eastward IMF electric field, which contributes to the plasmaspheric drainage plume, through the low-latitude ionosphere. In order to investigate temporal density variations of the inner plasmasphere when Polar observed the drainage plume connected the magnetopause, we have compared the dayside FLR-inferred equatorial densities at $L = 2.3$ and 2.9 during the main phase of the 11 April 2001 magnetic storm and before the storm. We obtained similar density profiles during the main phase of the storm and before the storm. This indicates that there is no significant density increase or decrease in the plasmasphere even though the nightside plasmapause moved inward by 1–2 R_E (see Figures 5 and 7) and the dayside plasmapause moved sunward as far outward as $L \approx 6$ (see Figure 4). *Goldstein et al.* [2003a] showed that the inward motion of the plasmapause in the nightside is not due to a global compression but erosion, stripping away of outer layers of the plasmasphere. The density in the plume region measured by Polar at $L \approx$ ~5.5–6 was 100–300 cm^{-3}, which is lower than the density in the plasmasphere inside $L = 2.9$ by a factor of ~1–2. This plume density is comparable to the density in the outer plasmasphere (L = ~4) [e.g., *Takahashi et al.*, 2001]. Thus, we suggest that the plasmaspheric plasma observed at Polar is eroded from the outer layers (L >3) of the plasmasphere. This indicates that the sunward convection of the plasmaspheric plasma does not deplete all L shells.

[26] In summary, Polar observed the cold, dense plasma attached to the magnetopause compressed inward by $L \approx 6$ in the prenoon (~1000–1100 MLT) sector during the early main phase of the geomagnetic storm on 11 April 2001. Using simultaneous solar wind and IMAGE/EUV observations, we confirmed that the cold, dense plasma enhancement observed by Polar was due to an erosion of the plasmasphere causing sunward motion of plasmaspheric plasma, i.e., inward on the nightside and outward on the dayside. That is, Polar observed a plasmaspheric drainage plume connected to the magnetopause. We showed that the ground stations ($L = 2.9$) with magnetic foot points whose MLT was inside the MLT range of the plume (see Figure 7) observed no significant difference in the mass density between the quiet time interval and storm time interval (see Figure 6). These observations suggest that the source of the plasmaspheric plasma of the plume is not inside L = 2.9, but the plume plasma came from outside $L = 2.9$. Although there are many observational studies about

dynamic behaviors of the plasmasphere during plasmaspheric erosions, our study is the first to show simultaneous magnetopause and imaging observations of a plume in the process of erosion to the best of the authors' knowledge.

[27] **Acknowledgments.** We thank MEASURE magnetometer team (http://measure.igpp.ucla.edu).We also thank H. Singer for the GOES magnetic field data. The Polar magnetic field data are provided at http://ssc.igpp.ucla.edu/forms/polar/. The HYDRA and spacecraft potential data from the Polar satellite are provided by the NASA's CDAWeb site (http://rumba.gsfc.nasa.gov/cdaweb/). The key parameter solar wind and magnetic field data of the ACE satellite are provided by the NASA's CDAWeb site. The *Dst* index data were provided by World Data Center C2 (WDC-C2) for Geomagnetism, Kyoto University. This work has been supported by the MOST grants(M1-0104-00-0059 and M1-0407-00-0001) of the Korean government. Work at Southwest Research Institute was generously supported by the NASA Sun-Earth Connections Guest Investigator program under NAG5-12787 and by the NASA IMAGE mission under NAS5-96020. D. B. was supported by NASA grant NGT5-117 and MEASURE is supported by NSF grant ATM-0196223.

[28] Zuyin Pu thanks the reviewers for their assistance in evaluating this paper.

References

Berube, D., M. B. Moldwin, and J. M. Weygand (2003), An automated method for the detection of field line resonance frequencies using ground magnetometer techniques, *J. Geophys. Res.*, *108*(A9), 1348, doi:10.1029/2002JA009737.

Berube, D., M. B. Moldwin, S. F. Fung, and J. L. Green (2005), A plasmaspheric mass density model and constraints on its heavy ion concentration, *J. Geophys. Res.*, *110*, A04212,doi:10.1029/2004JA010684.

Burch, J. L. (2000), IMAGE mission overview, *Space Sci. Rev.*, *91*, 1.

Carpenter, D. L. (1967), Relation between the dawn minimum in the equatorial radius of the plasmapause and Dst, Kp, and local K at Byrd station, *J. Geophys. Res.*, *72*, 2969.

Carpenter, D. L., and R. R. Anderson (1992), An ISEE/Whistler model of equatorial electron density in the magnetosphere, *J. Geophys. Res.*, *97*, 1097.

Carpenter, D. L., et al. (1993), Plasmasphere dynamics in the duskside bulge region: A new look at an old topic, *J. Geophys. Res.*, *98*, 19,243.

Carpenter, D. L., and J. Lemaire (1997), Erosion and recovery of the plasmasphere in the plasmapause region, *Space Sci. Rev.*, *80*, 153.

Chappell, C. R., K. K. Harris, and G. W. Sharp (1970), A study of the influence of magnetic activity on the location of the plasmapause as measured by OGO 5, *J. Geophys. Res.*, *75*, 50.

Chen, S.-H., and T. E. Moore (2006), Magnetospheric convection and thermal ions in the dayside outer magnetosphere, *J. Geophys. Res.*, *111*, A03215, doi:10.1029/2005JA011084.

Chi, P. J., C. T. Russell, S. Musman, W. K. Peterson, G. Le, V. Angelopolous, G. D. Reeves, M. B. Moldwin, and F. K. Chun (2000), Plasmaspheric depletion and refilling associated with theSeptember 25, 1998 magnetic storm observed by ground magnetometersat L = 2, *Geophys. Res. Lett.*, *27*, 633.

Chi, P. J., C. T. Russell, J. C. Foster, M. B. Moldwin, M. J. Engerbretson, and I. R. Mann (2005), Density enhancement in plasmasphere-ionosphere plasma during the Halloween superstorm: Observations along the 330th magnetic meridian in North America, *Geophys. Res. Lett.*, *32*, L03S07, doi:10.1029/2004GL021722.

Cummings, W. D., R. J. O'Sullivan, and P. J. Coleman Jr. (1969), Standing Alfvén waves in the magnetosphere, *J. Geophys. Res.*, *74*, 778.

Elphic, R. C., L. A. Weiss, M. F. Thomsen, and D. J. McComas (1996), Evolution of plasmaspheric ions at geosynchronous orbit during times of high geomagnetic activity, *Geophys. Res. Lett.*, *23*, 2189.

Elphic, R. C., M. F. Thomsen, and J. E. Borovsky (1997), The fate of the outer plasmasphere, *Geophys. Res. Lett.*, *24*, 365.

Goldstein, J., and B. R. Sandel (2005), The global pattern of evolution of plasmaspheric drainage plumes, in *Inner Magnetosphere Interactions: New Perspectives from Imaging*, Geophys. Monogr. Ser., vol. 159, edited by J. L. Burch, M. Schulz, and H. Spence, American Geophysical Union, Washington, D.C, doi:10.1029/2004BK000104.

Goldstein, J., B. R. Sandel, W. T. Forrester, and P. H. Reiff (2003a), IMF-driven plasmasphere erosion of 10 July 2000, *Geophys. Res. Lett.*, *30*(3), 1146, doi:10.1029/2002GL016478.

Goldstein, J., M. Spasojević, P. H. Reiff, B. R. Sandel, D. L. Gallagher, and B. W. Reinisch (2003b), Identifying the plasmapause in IMAGE EUV data using IMAGE RPI in situ steep density gradients, *J. Geophys. Res.*, *108*(A4), 1147, doi:10.1029/2002JA009475.

Goldstein, J., B. R. Sandel, M. R. Hairston, and S. B. Mende (2004a), Plasmapause undulation of 17 April 2002, *Geophys. Res. Lett.*, *31*, L15801, doi:10.1029/2004GL019959.

Goldstein, J., B. R. Sandel, M. F. Thomsen, M. Spasojević, and P. H. Reiff (2004b), Simultaneous remote sensing and in situ observations of plasmaspheric drainage plumes, *J. Geophys. Res.*, *109*, A03202, doi:10.1029/2003JA010281.

Goldstein, J., B. R. Sandel, W. T. Forrester, M. F. Thomsen, and M. R. Hairston (2005), Global plasmasphere evolution 22–23 April 2001, *J. Geophys. Res.*, *110*, A12218, doi:10.1029/2005JA011282.

Grebowsky, J. M. (1970), Model study of plasmapause motion, *J. Geophys. Res.*, *75*, 4329.

Higel, B., and L. Wu (1984), Electron density and plasmapause characteristics at 6.6 RE: A statistical study of GEOS 2 relaxation sounder data, *J. Geophys. Res.*, *89*, 1583.

Keiling, A., J. R. Wygant, C. Cattell, K.-H. Kim, C.T. Russell, D. K. Milling, M. Temerin, F. S. Mozer, and C. A. Kletzing (2001), Pi2 pulsations observed with the Polar satellite and ground stations: Coupling of trapped and propagating fast mode waves to a midlatitude field line resonance, *J. Geophys. Res.*, *106*(A11), doi:10.1029/2001JA900082.

Lemaire, J. F. and K. I. Gringauz (1998), *The Earth's Plasmasphere*, Cambridge Univ. Press, New York.

Moldwin, M. B., M. F. Thomsen, S. J. Bame, D. J. McComas, and K. R. Moore (1994), An examination of the structure and dynamics of the outer plasmasphere using multiple geosynchronous satellites, *J. Geophys. Res.*, *99*, 11,475.

Moldwin, M. B., L. Downward, H. K. Rassoul, R. Amin, and R. R. Anderson (2002), A new model of the location of the plasmapause: CRRES results, *J. Geophys. Res.*, *107*(A11), 1339, doi:10.1029/2001JA009211.

Pedersen, A. (1995), Solar wind and magnetosphere plasma diagnostics by spacecraft electrostatic potential measurements, *Ann. Geophys.*, *13*, 118.

Reinisch, B. W., X. Huang, P. Song, J. L. Green, S. F. Fung, V. M. Vasyliunas, D. L. Gallagher, and B. R. Sandel (2004), Plasmaspheric mass loss and refilling as a result of a magnetic storm,, *J. Geophys. Res.*, *109*, A01202, doi:10.1029/2003JA009948.

Sandel, B. R., et al. (2000), The extreme ultraviolet imager investigation for the IMAGE mission, *Space Sci. Rev.*, *91*, 197.

Sandel, B. R., R. A. King, W. T. Forrester, D. L. Gallagher, A. L. Broadfoot, and C. C. Curtis (2001), Initial results from the IMAGE extreme ultraviolet imager, *Geophys. Res. Lett.*, *28*, 1439.

Scudder, J. D., et al. (1995), Hydra-A 3-dimensional electron and ion hot plasma instrument for the Polar spacecraft of the GGS mission, in, *Space Sci. Rev.*, *71*, 495.

Scudder, J. D., X. Cao, and F. S. Mozer (2000), Photoemission current-spacecraft voltage relation: Key to routine, quantitative low-energy plasma measurements, *J. Geophys. Res.*, *105*(A9), doi:10.1029/1999JA900423.

Spasojević, M., J. Goldstein, D. L. Carpenter, U. S. Inan, B. R. Sandel, M. B. Moldwin, and B. W. Reinisch (2003), Global response of the plasmasphere to a geomagnetic disturbance, *J. Geophys. Res.*, *108*(A9), 1340, doi:10.1029/2003JA009987.

Su, Y.-J., J. E. Borovsky, M. F. Thomsen, R. C. Elphic, and D. J. McComas (2000), Plasmaspheric material at the reconnecting magnetopause, *J. Geophys. Res.*, *105*(A4), doi:10.1029/1999JA000266.

Su, Y.-J., J. E. Borovsky, M. F. Thomsen, N. Dubouloz, M. O. Chandler, T. E. Moore, and M. Bouhram (2001), Plasmaspheric material on high-latitude open field lines, *J. Geophys. Res.*, *106*(A4), doi:10.1029/2000JA003008.

Taguchi, S., M. R. Collier, T. E. Moore, M.-C. Fok, and H. J. Singer (2004), Response of neutral atom emissions in the low-latitude and high-latitude magnetosheath direction to the magnetopause motion under extreme solar wind conditions, *J. Geophys. Res.*, *107*, A04208, doi:10.1029/2003JA010147.

Takahashi, K., S.-I. Ohtani, W. J. Hughes, and R. R. Anderson (2001), CRRES observation of Pi2 pulsations: Wave mode inside and outside the plasmasphere, *J. Geophys. Res.*, *106*, 15,567.

Waters, C. L., F. W. Menk, and B. J. Fraser (1994), Low latitude geomagnetic field line resonance: Experiment and modeling, *J. Geophys. Res.*, *99*, 17,547.

D. Berube, Department of Earth and Space Sciences, Institute of Geophysics and Planetary Physics, University of California, Los Angeles, 595 Charles Young Drive E, Los Angeles, CA 90095-1567, USA. (dberube@igpp.ucla.edu)

J. Goldstein, Space Science and Engineering Division, Southwest Research Institute, 6220 Culebra Rd., San Antonio, TX 78228, USA. (jgoldstein@swri.edu)

K.-H. Kim, Korea Astronomy and Space Science Institute, Whaam-Dong, Youseong-Gu, Daejeon 305-348, Korea. (khan@kasi.re.kr)